Fast Stochastic Librations and Slow Rotations of Spin Labeled Stearic Acids in a Model Phospholipid Bilayer at Cryogenic Temperatures

ARTICLE *in* THE JOURNAL OF PHYSICAL CHEMISTRY B · NOVEMBER 2008

Impact Factor: 3.3 · DOI: 10.1021/jp805794c · Source: PubMed

2 AUTHORS:

Nikolay P. Isaev
Institute of Chemical Kinetics and Combus…
14 PUBLICATIONS **73** CITATIONS
SEE PROFILE

Sergei A Dzuba
Russian Academy of Sciences
111 PUBLICATIONS **1,684** CITATIONS
SEE PROFILE

Fast Stochastic Librations and Slow Rotations of Spin Labeled Stearic Acids in a Model Phospholipid Bilayer at Cryogenic Temperatures

Nikolay P. Isaev[†,‡] **and Sergei A. Dzuba***[,†,‡]

Institute of Chemical Kinetics and Combustion, Institutskaya-3, 630090 Novosibirsk, Russia, and Novosibirsk State University, 630090, Pirogova-2, Novosibirsk, Russia

Received: July 2, 2008; Revised Manuscript Received: August 21, 2008

The spin label DOXYL (4,4-dimethyl-oxazolidine-1-oxyl) is a nitroxyl ring that can be attached rigidly at specific C-atom positions in the stearic acid. 5-DOXYL-stearic acid and 16-DOXYL-stearic acid in 1-Palmitoyl-2-oleoyl-*sn*-glycero-3-phosphocholine (POPC) lipid bilayers were studied using electron spin echo (ESE) spectroscopy at low temperatures. The anisotropy of ESE decay across the electron paramagnetic resonance (EPR) spectrum evidence that these spin labels participate in orientational motions at temperatures down to ~120 K for 5-DOXYL-stearic acid and down to ~80 K for 16-DOXYL-stearic acid. Fast stochastic librations, with correlation time at the nanosecond time scale, manifest itself in a two-pulse ESE experiment. Stimulated three-pulse ESE experiment is sensitive to motions of ultrasmall amplitude, $\sim 0.1-1°$, developing at the microsecond time scale. The stimulated ESE decays were found to depend on the product of the two time delays of the pulse sequence. This fact may be described within a simple model of slow inertial rotations developing within this small range of angles with a rate of ~1 kHz. Both types of motion evidence the pronounced motional heterogeneity across the bilayer at cryogenic temperatures, with a remarkable increase of motion in the bilayer interior. The found low-temperature motions imply that hydrophobic parts of amphiphilic biomolecules may possess a noticeable mobility even at temperatures as low as ~100 K.

Introduction

The dynamics of molecules in biological membranes are of the crucial importance for their functioning. Studies of molecular motions in biological membranes at cryogenic temperatures may allow detecting motions across low energetic barriers, which inevitably present, but cannot manifest itself at physiological temperatures. Low-temperature dynamics in membranes have been studied employing neutron scattering,[1,2] nuclear magnetic resonance (NMR),[3,4] dielectric relaxation,[5] and other techniques. Also, studies of biological objects at low temperatures are currently the subject of intensive research because of the relevance to cryopreservation of biological tissues.[6]

Restricted small-amplitude stochastic orientational motions occurring at the nanosecond time scale (stochastic librations) in the membranes may be studied using electron spin echo (ESE) spectroscopy of spin-labeled lipids and other biomolecules embedded into membranes.[7−11] Nitroxide spin labels possess anisotropy of *g*-factor and of hyperfine interactions, which results in anisotropically broadened electron paramagnetic resonance (EPR) spectra. In pulsed EPR, the excitation bandwidth that is determined by microwave amplitude normally is much smaller than the total EPR line width. Such selective excitation applied to spectral positions of different degree of anisotropy provides the possibility of studying the anisotropy of spin relaxation. For nitroxides in organic glasses,[12,13] anisotropic relaxation seen in a two-pulse ESE experiment was explained within a framework of a model of stochastic librations near an equilibrium position, with correlation time τ_c much less than the time window of the ESE experiment. The latter is determined by the typical for organic solids value of the transverse spin relaxation time, $T_2 \sim 10^{-7}-10^{-6}$ s. The same model was applied later for spin labels in membranes.[7−11]

Stimulated three-pulse ESE experiment is sensitive to stochastic motions showing up at the microsecond time scale[14,15] which is determined by spin−lattice relaxation time, T_1. Orientational jumps larger than $\sim 2°$ may be studied using excitation performed near canonical orientations where anisotropy is small.[14] The study of motions of ultrasmall amplitudes, $\sim 0.1-1°$, employs excitation at the spectral positions between canonical orientations, where the anisotropy is high.[15] (This evaluation immediately follows from the characteristic anisotropy of nitroxide EPR spectra, that is around 5×10^8 s^{-1}, which at the microsecond time scale results in acquired phase around unity for the angle of ~0.1°.)

Such small-amplitude orientational molecular motions developing at the microsecond time scale cannot be detected with any other technique. These motions were found to manifest itself for spin probes in simple organic glass formers near their glass transition temperature, T_g.[15] Biological membranes are also known to possess properties of glassy system,[2,16] and are characterized by T_g around 200 K. Therefore, one may expect these motions showing up at low temperatures in biological membranes as well.

In this study we employ spin labeled 5-DOXYL-stearic acid and 16-DOXYL-stearic acid embedded into a model lipid bilayer. These spin labels are often used to study molecular dynamics in biological membranes.[17] As stearic acid molecules are expected to align along the lipid molecules of the bilayer with their polar terminuses located in the region of polar heads of lipid molecules, the use of different positions of the nitroxide fragment along the alkyl chain allows investigating molecular dynamics at different depths into the bilayer.

* Corresponding author. E-mail: dzuba@ns.kinetics.nsc.ru.
† Institute of Chemical Kinetics and Combustion.
‡ Novosibirsk State University.

10.1021/jp805794c CCC: $40.75
Published on Web 10/01/2008

Spectral Diffusion in Solids and Stimulated Echo

Stimulated ESE is formed after application of three microwave $\pi/2$ pulses to a spin system stored along the external magnetic field, in a time sequence denoted as $\pi/2-\tau-\pi/2-T-\pi/2-\tau-echo$. Echo signal $E(2\tau+T)$ decays with the time constant T_2 during the two τ-intervals and with the time constant T_1 during the T-interval:

$$E(2\tau+T) \propto \exp\{-2\tau/T_2 - T/T_1\} \quad (1)$$

Stochastic orientational motion in solids produces in anisotropically broadened spectra a stochastic fluctuation of the resonance frequency, $\Delta\omega(t)$, (spectral diffusion). If motion occurs via uncorrelated large-scale jumps with correlation time τ_c, then in the case of selective excitation each jump results in the irreversible loss of echo intensity:

$$E(2\tau+T) \propto \exp\{-(2\tau+T)/\tau_c\} \quad (2)$$

Note that it follows from the above simple relation between the excursion angle and the resonance frequency shift that, e.g., for a ~6 G excitation bandwidth the large-scale jumps mean jumps larger than ~10° amplitude.

In the alternative case of small-scale motions that result in spectral diffusion within the excitation bandwidth only, the echo signal decay is[18]

$$E(2\tau+T) \propto \left\langle \exp\left(-i\int_0^{\tau} \mathrm{d}t\, \Delta\omega(t)\right) \exp\left(i\int_{\tau+T}^{2\tau+T} \mathrm{d}t\, \Delta\omega(t)\right)\right\rangle \quad (3)$$

where angular brackets denote averaging over a stochastic trajectory. The two-pulse echo formally corresponds to the case $T = 0$.

If spectral diffusion due to stochastic motions is fast ($\tau_c < \tau$), eq 3 results in an exponential decay[18,19]

$$E(2\tau+T) \propto \exp(-2\tau\tau_c\langle\Delta\omega^2(t)\rangle) \quad (4)$$

provided that the $\langle\Delta\omega^2(t)\rangle$ exists. Note that the right-hand part of eq 4 does not depend on T.

For the mechanism of unrestricted Brownian spectral diffusion (but still developing within the excitation bandwidth) via infinitesimal steps in the frequency space echo decays as[19]

$$E(2\tau+T) \propto \exp\left(-D_\omega\left(\frac{2}{3}\tau^3 + \tau^2 T\right)\right) \quad (5)$$

where D_ω is the diffusion coefficient in the frequency space. To turn to diffusion of nitroxide spin label in the angular space, let us simplify the problem by assuming the axial symmetry of the g-tensor of nitroxide and that of the hyperfine interaction tensor (normally this approximation is acceptable). Molecular framework is determined by the axes where both tensors are diagonal, with the Z axis along the axial symmetry axis. For small angles $\alpha(t)$ of motion around the X molecular axis the linear relation takes place:[13]

$$\Delta\omega(t) \cong \alpha(t) R_m(\theta,\phi) \quad (6)$$

where

$$R_m(\theta,\phi) = \gamma\left[B(g_\perp - g_\parallel) + \frac{m(A_\perp^2 - A_\parallel^2)}{(A_\perp \sin^2\theta + A_\parallel^2 \cos^2\theta)^{1/2}}\right] \times \sin\theta\cos\theta\sin\phi$$

where in turn θ and φ are the angles determining the orientation of the magnetic field in the molecular framework, B is the magnetic field strength, $g_\parallel$, $g_\perp$, $A_\parallel$, and $A_\perp$ are the principal values of the g-tensor and the tensor of hyperfine interaction, and m is the nitrogen nucleus spin projection onto its quantization axis. For small-angle motions angles θ and φ in (6) may be considered as constant. The m value for the case of selective excitation also may be considered as a constant, because nuclear spin flips result in this case in a slow large-scale spectral diffusion, which may be taken into account by eq 2. Then instead of (5) we have

$$E(2\tau+T) \propto \exp\left(-R_m^2(\theta,\phi) D_X\left(\frac{2}{3}\tau^3 + \tau^2 T\right)\right) \quad (7)$$

where D_X is the diffusion coefficient in the angular space, for motion around the X molecular axis. Note that $R_m(\theta,\varphi)$ here plays a role of the field gradient that is applied artificially in the NMR studies of molecular diffusion.[19]

For motion around the Y molecular axis sin φ in (6) is replaced by cos φ. Motion around the Z molecular axis under the used axial approximation does not produce spectral diffusion.

For reorientations within a small range of angles (~0.1−1°) the model of infinitesimal steps in the angular space may be not appropriate. Instead, a model of inertial rotations, in which the molecule freely rotates with an angular velocity Ω during some time interval,[20,21] seems to be physically more reasonable. For this simple model from eq 3, we have:

$$E(2\tau+T) \propto \int \cos\{R_m(\theta,\phi)\Omega(\tau^2 + \tau T)\} g(\Omega)\, \mathrm{d}\Omega \quad (8)$$

where $g(\Omega)$ is the distribution function for angular velocities.

The unique property of formula 8 is its dependence on the multiplication of the two time delays, τ and T (cf. eqs 1, 2, 4, and 7). Note that normally in experiment $T \gg \tau$, so the term proportional to τ^2 in eq 8 is not important.

As different mechanisms may be considered to be independent, the decay is determined by multiplication of the different factors discussed above. In that relation, it is possible to easily discard the contribution presented by eqs 1 and 2. Indeed, all isotropic relaxation processes may be eliminated by comparing echo decays obtained for the field positions with different spectral anisotropy (i.e., where $R_m(\theta,\varphi)$ is different). And, the analysis of the logarithm of echo amplitude as a function of τ with T fixed, allows refining only the τ-dependent processes and discarding spin−lattice relaxation and slow ($\tau_c > \tau$) large-scale spectral diffusion (see eqs 1 and 2).

Note that all above formulas, except eq 4, are valid only when $T = 0$ and/or when $T \gg T_2$. In the intermediate region, $T \sim T_2$, the transverse relaxation during the T-interval also contributes to the echo decay. To avoid this complication, one should exclude these data from consideration.

Echo decay may be influenced also by a so-called instantaneous spectral diffusion,[18] which is induced by spin flips under the action of microwave pulses that modulates the magnetic dipole−dipole interactions between electron spins of different nitroxides, if the nitroxide concentration is high.

Experimental Section

The spin-labeled 5-DOXYL-stearic acid and 16-DOXYL-stearic acid (DOXYL is 4,4-dimethyl-oxazolidine-1-oxyl) were used in this work (Fluka):

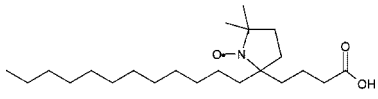

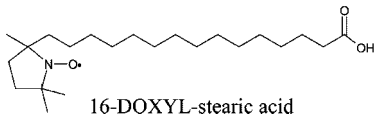

These acids were dissolved in chloroform with 1-palmitoyl-2-oleoyl-*sn*-glycero-3-phosphocholine (POPC) lipids (Aldrich) at a 1:100 molar ratio, and the solution was then spread on a glass plate. The solvent was removed by evaporation in vacuum. Then the sample was hydrated at room temperature by water vapors of 100% humidity.

A Bruker ELEXSYS E580 X-band FT EPR spectrometer was used equipped with a dielectric cavity (Bruker ER 4118 X-MD-5) inside an Oxford Instruments CF 935 cryostat. Duration of microwave pulses was 16 ns and their amplitudes were adjusted to provide a $\pi/2$ turning angle (so making the amplitude ~6 G). Cryostat was cooled either by cold nitrogen or by cold helium. The sample temperature was monitored with a calibrated Cu−constantan thermocouple directly placed into the sample tube. Temperature was maintained with an accuracy of ±0.5 K.

Results

Continuous wave (CW) EPR spectra are given in Figure 1 for both samples in two orientations—with the magnetic field parallel and perpendicular to the normal of the sample surface, at room temperature and at 94 K. One can see a remarkable anisotropy of EPR spectra in all cases. For the case of 5-DOXYL-stearic acid, this anisotropy is larger than for the case of 16-DOXYL-stearic acid. At 94 K EPR spectra of both samples are immobilized. At room temperature the EPR spectra for the 5-DOXYL-stearic acid are almost immobilized while those for the 16-DOXYL-stearic acid show fast motion.

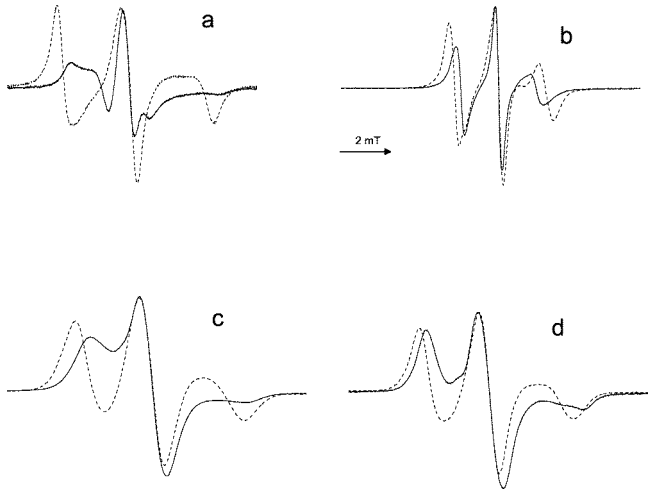

Figure 1. Continuous wave EPR spectra at room temperature (a, b) and at 94 K (c, d) for 5-DOXYL-stearic acid (a, c) and for 16-DOXYL-stearic acid (b, d) in POPC bilayer, for the orientations of the bilayer normal parallel (solid line) and perpendicular (dashed line) respectively to the magnetic field.

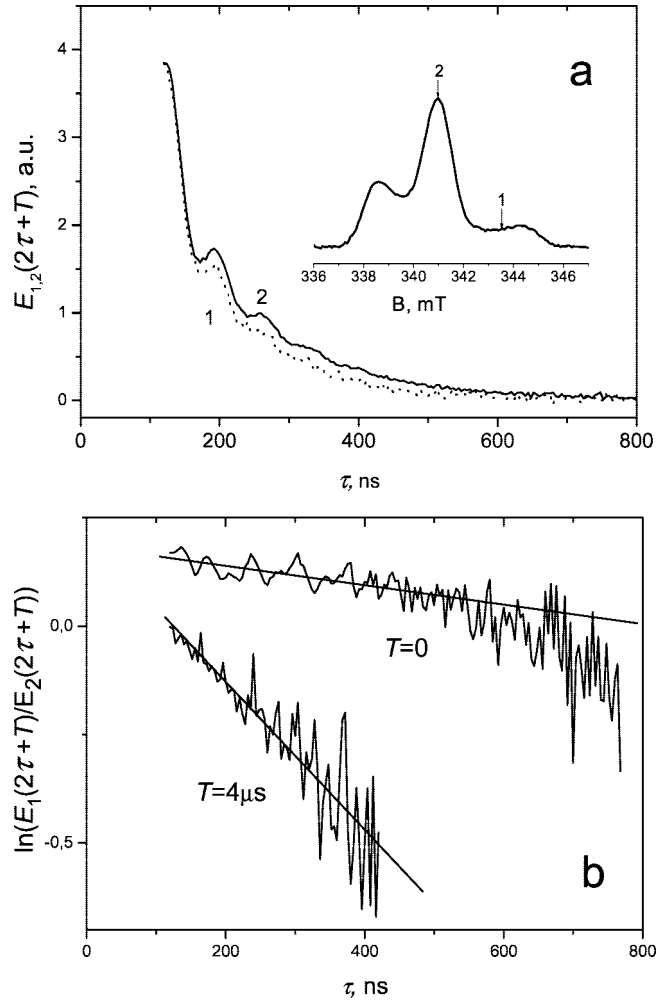

Figure 2. (a) Echo decay traces vs τ for $T = 4$ μs, for two field positions shown in insert. The intensities at beginning are artificially adjusted approximately to the same value. (b) semilogarithmic plot of the ratio of these traces and of traces taken at the time delay $T = 0$. The linear approximations of these ratios also are shown. For convenience, data are shifted arbitrarily along the vertical axis. The temperature is 145 K; the sample is 5-DOXYL-stearic acid in perpendicular orientation.

The higher degree of anisotropy for the fifth label position as compared with the 16th one proves that stearic acid molecules are indeed embedded in the bilayer along the lipid molecules, as it is expected in this case.

Echo decays in our experiments were recorded for two different positions in the EPR spectrum indicated by arrows in the insert to Figure 2a, where a two-pulse echo amplitude is given vs scanning magnetic field, with the time delay τ fixed (a so-called echo-detected EPR line shape). These two positions correspond to two limiting cases of the anisotropy of magnetic interactions in the EPR spectrum—the highest one for the first position, and the lowest one for the second position. One can see from Figure 2a that larger anisotropy results in a faster decay. This means that orientational motion indeed contributes to the echo decay. The comparison of the decays at different positions provides the possibility to detect the motion.

Also, noticeable oscillations (ESE envelope modulation or ESEEM[22]) are seen at the decay curves.

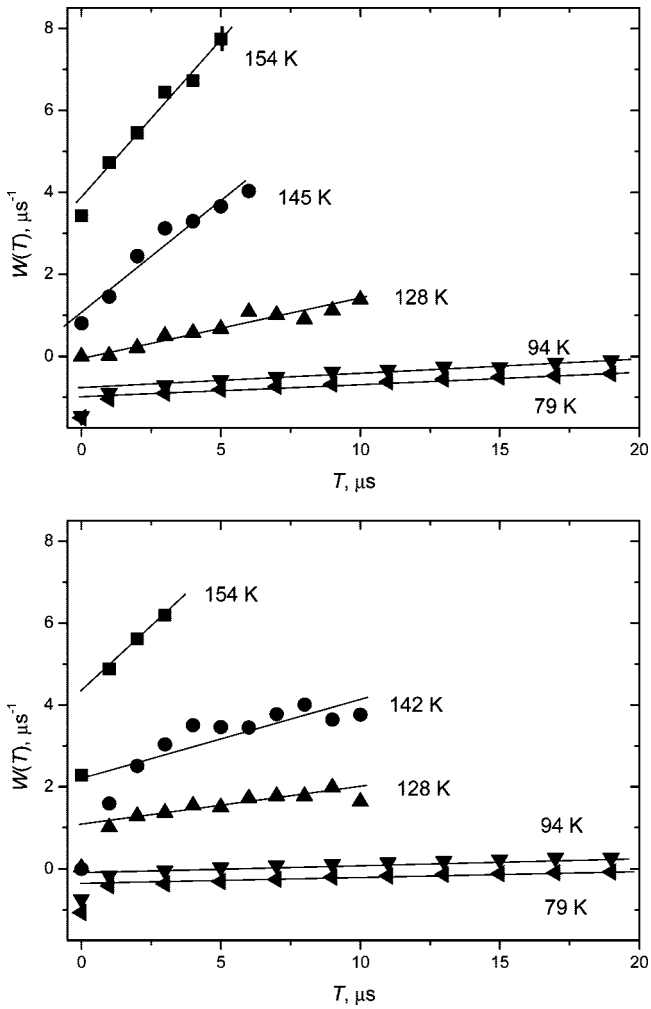

Figure 3. The relaxation rates $W(T)$ obtained from the slopes of straight lines, like those shown in Figure 2b, for 5-DOXYL-stearic acid in POPC bilayer at parallel (top) and perpendicular (bottom) orientation of the bilayer normal respectively to the magnetic field, as a function of the time delay T at different temperatures.

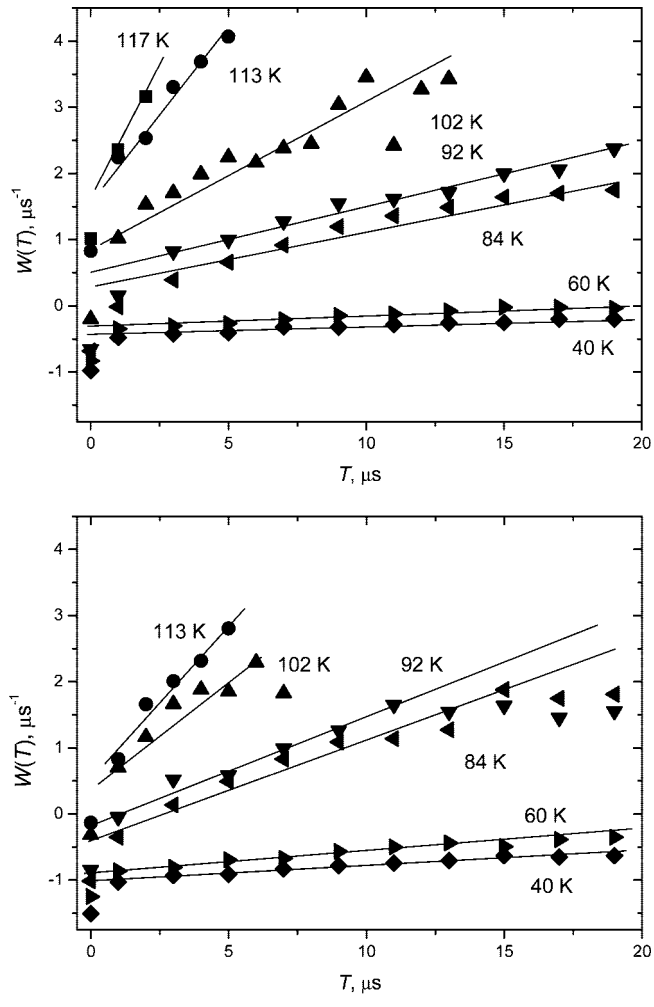

Figure 4. Same plots as in Figure 3, for 16-DOXYL-stearic acid in POPC bilayer.

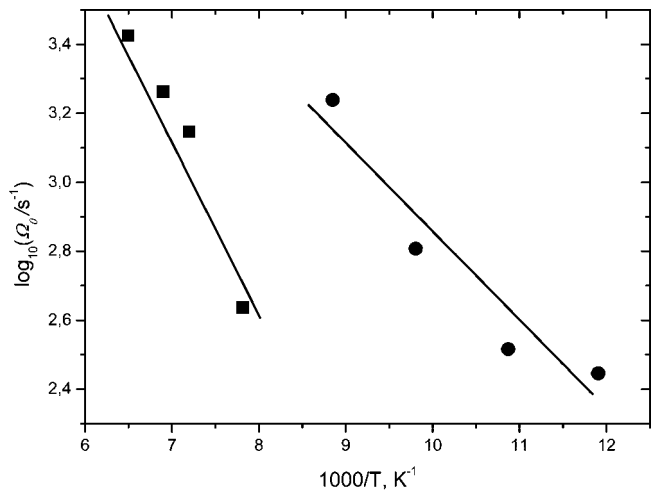

Figure 5. The rotational rates Ω_0 (see eq 9 for definition) for 5-DOXYL-stearic acid (squares) and for 16-DOXYL-stearic acid in POPC bilayer (circles). Lines are drawn to guide the eye.

To refine a pure contribution of anisotropic relaxation, we divided the time traces for the decays at the first field position by those at the second one. The results are given in Figure 2b in a semilogarithmic scale for two time delays, $T = 0$ and $T = 4\ \mu$s. Note that after division ESEEM oscillations are essentially damped (which means that they are field-independent). One can see that echo decay in the semilogarithmic scale is satisfactorily fitted by a straight line. The slope of the line we denote hereafter as $W(T)$. (For the $T = 0$ case, some indication on quadratic behavior is also seen in Figure 2b at large T.)

The echo signal for the two samples studied was found in two different temperature ranges - below 117 K for the 16-DOXYL-stearic acid sample and below 154 K for the 5-DOXYL-stearic acid sample. Above these temperatures the echo decay was too fast the signal to be observed.

The obtained fitting parameters, $W(T)$, are given vs T for different temperatures and systems studied: in Figure 3 for 5-DOXYL-stearic acid and in Figure 4 for 16-DOXYL-stearic acid, for parallel and perpendicular magnetic field orientations to the normal of the lipid bilayer surfaces. (One can see that there is no remarkable difference for the two orientations.)

The important feature seen in Figures 3 and 4 is that data in all cases may be satisfactorily described by linear dependences, possibly excluding the initial point $T = 0$ (the relation between the two-pulse and three-pulse experiments at $T \leq T_2$ is complicated, as was mentioned above). Recollecting that $W(T)$ is the rate of exponential decay on τ, this fact implies that echo decay exponentially depends on the time variables as $\exp(-a\tau + b\tau T)$, where a and b are some fitting parameters.

The experimental errors of data presented in Figures 3 and 4 are induced by temperature instability during the measurement

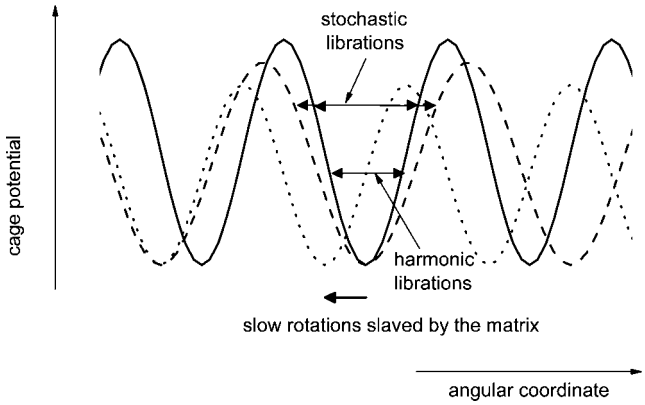

Figure 6. A possible scenario and the hierarchy of orientational motions of spin molecular probes in a bilayer. At low temperatures only harmonic librational motions are present in well-defined cage potentials (solid curve) formed by the surrounding lipids. These motions do not manifest itself in ESE experiment because of their high frequency. Increase of temperature results in the cage potential "breathing" (dashed curve), which makes the motion stochastic; this manifests itself in relaxation seen in two-pulse ESE experiment. And increase of temperature also induces the cage rearranging (dotted curve), which results in a slaved motion of the probe. This motion manifests itself in relaxation seen in three-pulse ESE experiment.

and also depend on the signal intensity; they approximately correspond to the data scattering seen in these figures. One can see that for higher temperatures the errors are larger.

For the mechanism of instantaneous spectral diffusion (see above) the echo decay at the first spectral position must be slower than that for the second one (see as an example data in ref 23). Instantaneous diffusion is the only possible reason for the negative values of the $W(T)$ parameter seen in Figures 3 and 4. As the instantaneous diffusion does not depend on temperature, the deviation of data at low temperatures from zero line (94 K in Figure 3 and 40−60 K in Figure 4) presents its pure contribution at any other temperature.

Discussion

According to data presented in Figure 1, at room temperature the motion of the spin label in 16-DOXYL-stearic acid is faster than motion of spin label in the 5-DOXYL-stearic acid. Also, two spin label positions along the alkyl chain exhibit different EPR spectra anisotropy: for the 5-DOXYL-stearic acid it is more pronounced than that for the 16-DOXYL-stearic acid. This behavior of the motion at room temperature and of the ordering is well-known for spin-labeled biological membranes—see, e.g. ref 24. Therefore, these data evidence that spin-labeled stearic acids are indeed stretched across the membrane.

While at cryogenic temperatures CW EPR spectra do not show motions (Figure 1c,d), pulsed EPR evidence the presence of intensive motions (Figures 3 and 4). A nonzero initial intercepts on the T-dependences in Figures 3 and 4 (results of two-pulse echo experiments) evidence the presence of fast stochastic librations which may be described by eq 4. Previously, in studies of simple molecular glass formers (glycerol and *o*-terphenyl)[25] the nature of motions at the nanosecond time scale was supposed to be the same as that of large-amplitude anharmonic (or stochastic) atomic vibrations seen in glasses by neutron scattering and Mössbauer absorption.[26−28] This assigning was based on the closeness of temperatures where the motions appear, on the similarities of their time scales (neutron scattering is sensitive to motions faster than 10^9 s^{-1} and Mössbauer absorption to motions faster than 10^7 s^{-1}), and on the comparability of the amplitudes of motions found in these techniques. The transition in glasses with temperature increase from harmonic to anharmonic (or stochastic) motions is called a dynamical transition.[26−28] In hydrated proteins, it occurs near 200 K.

The appearance with increasing temperature of an apparent dependence on T indicates on the onset of motions developing at the microsecond time scale. The linear behavior of the T-dependences seen in Figures 3 and 4 may be explained within the model of inertial rotations - see eq 8. For the rates Ω small enough (we consider here the case of slow rotations), so that the product $|R_m(\theta,\varphi)|\Omega(\tau^2 + \tau T)$ is also small, Eq. (8) may be approximately presented as

$$E(2\tau + T) \propto 1 - |R_m(\theta, \phi)|\Omega_0(\tau^2 + \tau T) \approx \exp(-|R_m(\theta, \phi)|\Omega_0(\tau^2 + \tau T)) \quad (9)$$

where Ω_0 is determined by the first term of Taylor expansion of the echo signal, $\Omega_0 \equiv [1/|R_m(\theta,\varphi)|][\mathrm{d}/\mathrm{d}(\tau^2 + \tau T)]E(2\tau + T)|_{(\tau^2+\tau T)} \rightarrow 0$. In the case of Lorentzian distribution of $g(\Omega)$ the parameter Ω_0 is equal to the half-width at the half-height of this distribution. (In this case the exponential dependence in eq 9 presents an exact result.)

Equation 9, multiplied by eq 4, provides the functional dependence of the type of $\exp(-a\tau + b\tau T)$, which is actually observed in the experiment (see above, the term proportional to τ^2 may be neglected).

Note that exponential behavior takes place only when $\Omega_0 \neq 0$. From eq 8, it follows that the necessary condition for that is the divergence of the second moment of the $g(\Omega)$ distribution (as it takes place for the Lorentzian distribution).

For determining the Ω_0 rate from the experiment, it is necessary to evaluate the $|R_m(\theta,\varphi)|$ values for the two field positions we used. Our numerical simulations of the echo decays at the first and second EPR spectral positions (see Figure 1a), in line with eq 9 (data not given, in simulations we used parameters $g_\perp - g_\parallel = 0.0050$, $B = 3400$ G, $A_\parallel = 35$ G and $A_\perp = 5$ G) have shown that $|R_m(\theta,\varphi)|$ in eq 9 may be replaced by a constant equal to $\sim 3 \times 10^8$ s^{-1}, for both orientations of the motional axes—along the X and the Y molecular axes. For motion around the Z molecular axis under the employed axial symmetry approximation relaxation does not occur. If we assume that motion takes place independently around all three molecular axes, the Ω_0 value obtained from comparison with experiment must be multiplied by a factor of $^3/_2$, to get the total rotation rate. This was obtained from data of Figures 3 and 4, and the total rotation rates are presented in Figure 5.

Note that the found values $\Omega_0 < 3 \times 10^3$ s (see Figure 5) mean that reorientation angles within our experimental time window (2×10^{-5} s) is less than 4°, which falls into the introduced above criterion of small-angle motions.

It is interesting to indicate on the difference between ESE data for spin probes in simple molecular glass formers[25] and the present data on lipid bilayers. Fast stochastic librations and slow rotations in molecular glasses appear at temperature near T_g. In bilayers both these types of motion appear well below T_g (as was mentioned above, T_g is around 200 K for lipid bilayers). Also, in molecular glasses the onset of fast stochastic librations occurs at temperatures distinctly lower than temperatures where slow rotations appear. But for lipid bilayers both temperatures are close—see Figures 3 and 4.

The presence of fast motions at cryogenic temperatures found here is in agreement with the analogous data on spin-labeled molecules of different type in lipid bilayers. For spin-labeled

lipids in dipalmitoyl phosphatidylcholine (DPPC) bilayers,[10] for the label positions in the bilayer interior fast motions were found above ~100 K. Also, like here, motional heterogeneity was found—when deeper into the membrane, the motion is faster.[10] For cholestane spin label in dimyristoyl phosphatidylcholine (DMPC) bilayer[7] stochastic librations were found below 170 K. For spin-labeled peptide–antibiotic alamethicin in DMPC bilayer, stochastic librations are seen above 100 K.[11]

As the presented approach probes the motion developing at the microsecond time scale within an extremely small range of angles, data of other techniques available in literature hardly may be used here for comparison. A conventional NMR approach is not sensitive to motions at this range, and low-temperature measurements of motion in lipid bilayers were done with NMR above ~220 K.[3,4] Dielectric relaxation data at low temperatures also are scarce. For purple membranes that consist of the membrane protein bacteriorhodopsin (75% w/w) and lipid molecules (25% w/w) dielectric relaxation data[5] indicate on fast motions at low temperatures, well below glass transition. The investigation by neutron scattering of nanosecond molecular dynamics in purple membranes[1,2] has revealed a pronounced dynamical transition near 200 K[1] or near 150 K.[2]

Note that to relate the obtained Ω_0 parameter with the rotational diffusion coefficient, additional information on the distribution function $g(\Omega)$ is required, as well as on the distribution of correlation times. This could be a subject of further studies. But Ω_0 could serve as a parameter for comparison with theoretical models.

We also note that neutron scattering data on proteins indicate on an additional dynamical transition in ns time scale for atomic vibrations occurring near 100 K.[29−33] It is ascribed usually to methyl group rotation. In this work we observe stochastic librations at the ns time scale also appearing near 100 K (manifesting itself in Figure 4 as the appearance of nonzero intercepts). In our experiments the influence of methyl group on the dynamics of spin labels hardly could be important. Although in the vicinity of the unpaired electron in the spin label methyl groups indeed are attached, their rotation is not expected to contribute to anisotropic relaxation, as in experiments with nitroxide spin probes in molecular glasses[25] no relaxation was detected near 100 K. Probably, the observed fast stochastic motions could be an intrinsic property of large amphiphilic molecules in which system "architecture" is determined by strong interactions of the polar parts of the molecule while hydrophobic parts possess additional degrees of freedom allowing them to move freely even at low temperatures.

We may propose a possible scenario of orientational motions in bilayers at cryogenic temperatures, which is consistent with the all data set obtained with ESE of molecular spin probes—see Figure 6. Spin label moves in a cage potential, created by interaction with surrounding lipid molecules. Below ~90 K for the fifth label position and below ~60 K for the 16th label position only harmonic librational motions in a well-defined cage potential are present, which do not manifest itself in ESE experiment because of high-frequency of these motions.[13] Increasing temperature results in a potential "breathing", which makes the motion stochastic, the latter manifests itself in relaxation seen in two-pulse ESE experiment above ~90 K for the fifth label position and above ~60 K for the 16th label position. Slow inertial rotations, which manifests itself in relaxation seen in three-pulse ESE experiment above these temperatures, may appear as a result of the change of the local potential due to slow collective rearrangement of the lipids in the bilayer. (So the rotations are slaved by matrix motion.)

Conclusions

The results of the present study evidence that nitroxide spin probe molecules in POPC lipid bilayers participate in stochastic orientational motions down to very low temperatures, ~80 K for 16-DOXYL-stearic acid and ~120 K for 5-DOXYL-stearic acid.

The librational motions at the nanosecond time scale, which manifests itself in a two-pulse ESE experiment, may be related with atomic anharmonic vibrational motions in glasses seen in neutron scattering and Mössbauer absorption,[26−28] above temperature of a so-called dynamical transition. The temperatures where stochastic librations appear are found in this work to be much lower than those for spin labels in simple organic glass formers of comparable glass transition temperature (glycerol, $T_g = 185$ K, *o*-terphenyl, $T_g = 243$ K).[25] This indicates on the relative freedom in the membrane interior for chain packing as compared with molecular packing in organic glasses.

Stimulated ESE experiment for the approach used in this work is sensitive to stochastic motions of ultrasmall amplitude, ~0.1−1°, and developing in a microsecond time scale. The stimulated ESE decays in this work were found to depend on the product of the two time delays of the pulse sequence. This salient fact may be described within a simple model of slow inertial rotations within this small range of angles, developing at ~1 kHz frequency.

Both types of motion evidence the pronounced motional heterogeneity across the bilayer at cryogenic temperatures, with rapid increase of motion in the bilayer interior. The found low-temperature motions imply that hydrophobic parts of amphiphilic biomolecules may possess a noticeable mobility even at temperatures as low as ~100 K.

ESE data for two bilayer orientations in the magnetic field shows that the observed motions are isotropic. CW EPR electron paramagnetic resonance spectra indicate that ordering for 5-DOXYL-stearic acid is remarkably higher that that for 16-DOXYL-stearic acid. The molecular motions at room temperature are found from these spectra to be much faster in the latter case than in the former one.

Note the difference between data for simple molecular glass formers,[25] where fast stochastic librations were found to appear at temperature near T_g and slow rotations are found to appear at temperature somewhat above T_g, and present data on lipid bilayers, where both these type of motions appear well below T_g at nearly the same temperature.

Acknowledgment. This work was supported by the Civilian Research & Development Foundation (CRDF), No. RUC1-2635-NO-05, by the Russian Foundation for Basic Research, No. 08-03-00261, and by Siberian Branch of RAS (project No. 50).

References and Notes

(1) Fitter, J. *J. Phys. Chem. B.* **1999**, *103*, 8036.
(2) Weik, M.; Lehnert, U.; Zaccai, G. *Biophys. J.* **2005**, *89*, 3639.
(3) Meier, P.; Ohmes, E.; Kothe, G.; Blume, A.; Weiner, J.; Eibl, H.-J. *J. Phys. Chem.;* **1983**, *87*, 4904.
(4) Lehnert, R.; Eibl, H.-J.; Müller, K. *J. Phys. Chem. B* **2004**, *108*, 12141.
(5) Berntsen, P.; Bergman, R.; Jansson, H.; Weik, M.; Swenson, J. *Biophys. J.* **2005**, *89*, 3120.
(6) Fahy, G. M.; Wowk, B.; Wu, J.; Phan, J.; Rasch, C.; Chang, A.; Zendejas, E. *Cryobiology* **2004**, *48*, 157.

(7) Dzuba, S. A.; Watari, H.; Shimoyama, Y.; Maryasov, A. G.; Kodera, Y.; Kawamori, A. *J. Magn. Reson. A* **1995**, *115*, 80.

(8) Bartucci, R.; Guzzi, R.; Marsh, D.; Sportelli, L. *J. Magn. Reson.* **2003**, *162*, 371.

(9) Erilov, D. A.; Bartucci, R.; Guzzi, R.; Marsh, D.; Dzuba, S. A.; Sportelli, L. *J. Phys. Chem. B;* **2004**, *108*, 4501.

(10) Erilov, D. A.; Bartucci, R.; Guzzi, R.; Marsh, D.; Dzuba, S. A.; Sportelli, L. *Biophys. J.* **2004**, *87*, 3873.

(11) Bartucci, R.; Guzzi, R.; De Zotti, M.; Toniolo, C.; Marsh, D.; Sportelli, L. *Biophys. J.* **2008**, *94*, 2698.

(12) Dzuba, S. A. *Phys. Lett. A* **1996**, *213*, 77.

(13) Kirilina, E. P.; Dzuba, S. A.; Maryasov, A. G.; Tsvetkov, Yu. D. *Appl. Magn. Reson.* **2001**, *21*, 203.

(14) Leporini, D.; Schadler, V.; Wiesner, U.; Spiess, H. W.; Jeshke, G. *J. Chem. Phys.* **2003**, *119*, 11829.

(15) Dzuba, S. A.; Kirilina, E. P.; Salnikov, E. S.; Kulik, L. V. *J. Chem. Phys.* **2005**, *122*, 094702.

(16) Shalaev, E. Y.; Steponkus, P. L. *J. Phys. Chem. B* **2003**, *107*, 8734.

(17) Stimson, L.; Dong, L.; Karttunen, M.; Wisniewska, A.; Dutka, M.; Rog, T. *J. Phys. Chem. B* **2007**, *111*, 12453.

(18) Klauder, J. R.; Anderson, P. W. *Phys. Rev.* **1962**, *125*, 912.

(19) Abragam, A. *The Principles of Nuclear Magnetism*; Clarendon Press: Oxford, U.K., 1961.

(20) Valiev, K. A.; Ivanov, E. N. *Sov. Phys.-Usp.* **1973**, *16*, 1.

(21) Earle, K. A.; Budil, D. E.; Freed, J. H. *J. Phys. Chem.* **1993**, *97*, 13289.

(22) Dikanov, S. A.; Tsvetkov, Y. D. *Electron Spin Echo Envelope Modulation (ESEEM) Spectroscopy*; CRC Press: Boca Raton, FL, 1992.

(23) Toropov, Y. V.; Dzuba, S. A.; Tsvetkov, Y. D.; Monaco, V.; Formaggio, F.; Crisma, M.; Toniolo, C.; Raap, J. *Appl. Magn. Reson.* **1998**, *15*, 237.

(24) Fajer, P.; Watts, A.; Marsh, D. *Biophys. J.* **1992**, *61*, 879.

(25) Dzuba, S. A.; Kirilina, E. P.; Salnikov, E. S. *J. Chem. Phys.* **2006**, *125*, 054502.

(26) Wuttke, J.; Petry, W.; Coddens, G.; Fujara, F. *Phys. Rev. E* **1995**, *52*, 4026.

(27) Petry, W.; Bartsch, E.; Fujara, F.; Kiebel, M.; Sillescu, H.; Farago, B. *Phys. B: Condensed Matter* **1991**, *83*, 175.

(28) Tölle, A.; Zimmermann, H.; Fujara, F.; Petry, W.; Schmidt, W.; Schober, H.; Wuttke, J. *Eur. Phys. J. B* **2000**, *16*, 73.

(29) Lehnert, U.; Reat, V.; Weik, M.; Zaccai, G.; Pfister, C. *Biophys. J.* **1998**, *75*, 1945.

(30) Roh, J. H.; Novikov, V. N.; Gregory, R. B.; Curtis, J. E.; Chowdhuri, Z.; Sokolov, A. P. *Phys. Rev. Lett.* **2005**, *95*, 038101.

(31) Paciaroni, A.; Orecchini, A.; Cinelli, S.; Onori, G.; Lechner, R. E.; Pieper, J. *Chem. Phys.* **2003**, *292*, 397.

(32) Curtis, J. E.; Tarek, M.; Tobias, D. J. *J. Am. Chem. Soc.* **2004**, *126*, 15928.

(33) Pieper, J.; Hauss, T.; Buchsteiner, A.; Baczynski, K.; Adamiak, K.; Lechner, R. E.; Renger, G. *Biochemistry* **2007**, *46*, 11398.

JP805794C